Journal of Medicinal Chemistry

Article

pubs.acs.org/jmc

Detection of mRNA of the Cyclin D1 Breast Cancer Marker by a Novel Duplex-DNA Probe

Meirav Segal,[†] Eylon Yavin,[‡] Pinhas Kafri,[§] Yaron Shav-Tal,[§] and Bilha Fischer*,[†]

[†]Department of Chemistry, Bar-Ilan University, Ramat-Gan 52900, Israel

[‡]School of Pharmacy, Institute for Drug Research, The Hebrew University of Jerusalem, Ein Karem, Jerusalem 91120, Israel

[§]Faculty of Life Sciences and Institute of Nanotechnology, Bar-Ilan University, Ramat-Gan 52900, Israel

Supporting Information

ABSTRACT: Previously, we have described 5-((4-methoxy-phenyl)-*trans*-vinyl)-2′-deoxy-uridine, **6**, as a fluorescent uridine analogue exhibiting a 3000-fold higher quantum yield (Φ 0.12) and maximum emission (478 nm) which is 170 nm red-shifted as compared to uridine. Here, we utilized **6** for preparation of labeled oligodeoxynucleotide (ODN) probes based on MS2 and cyclin D1 (a known breast cancer mRNA marker) sequences. Cyclin D1-derived labeled-ssODN showed a 9.5-fold decrease of quantum yield upon duplex formation. On the basis of this finding, we developed the ds-NIF (nucleoside with intrinsic fluorescence)-probe methodology for detection of cyclin D1 mRNA, by which the fluorescent probe is released upon recognition of target mRNA by the relatively dark NIF-duplex-probe. Indeed, we successfully detected, a ss-deoxynucleic acid (DNA) variant of cyclin D1 mRNA using a dark NIF-labeled duplex-probe, and monitoring the recognition process by fluorescence spectroscopy and gel electrophoresis. Furthermore, we successfully detected cyclin D1 mRNA in RNA extracted from cancerous human cells, using ds-NIF methodology.

INTRODUCTION

The need to diagnose specific deoxynucleic acid (DNA) and ribonucleic acid (RNA) sequences has created a demand for recognition probes that respond with high signal-to-noise ratios and low fluorescence background.[1−3] For this purpose, various fluorescent nucleoside analogues[4−7] and oligonucleotide probes have been developed.[8,9] Most of these probes include extrinsic fluorescent dyes[10−12] for nucleic acid staining and labeling, intercalating dyes, and minor groove binding dyes. These dyes are used in various techniques for detecting genetic material in DNA arrays,[13] FISH,[14] gels,[15] virus particles,[16] and cells by fluorescence microscopy or electrophoresed gels.[17]

Methodologies using extrinsic fluorescent dyes are in many cases limited due to experimental procedures required prior to detection, poor solubility of dyes in water/phosphate buffer, toxicity of certain dyes, or background fluorescence of unreacted dyes. In addition, the large hydrophobic dye attached to a nucleotide alters the efficiency of enzymatic incorporation into DNA/RNA, resulting in different levels of labeling and prohibits quantification of nucleic acids. Even a two-step protocol involving first the incorporation of a slightly modified nucleotide into a nucleic acid, e.g., aminoallyl modified bases,[18] followed by covalent binding of fluorescent dyes, to allow the synthesis of multiply labeled fluorescent oligomer hybridization probes,[19] requires laborious multiple serial labeling and purifications to increase labeling and visualization efficiency.[20]

The limitations and complications of methodologies applying extrinsic dyes for nucleic acids detection emphasize the need for different fluorescent probes.

Over the past decade a number of nucleoside analogues with intrinsic fluorescence, replacing natural DNA bases in oligonucleotide probes, have been reported as an alternative to dye-substituted nucleosides.[21−26] For instance, pyrimidine nucleosides with intrinsic fluorescence include 5-methyl propargyl ether-2′-deoxyuridine,[23] **1**; 5-benzothiophene-uridine,[3] **2** (λ_{max} 318 nm, λ_{em} 458 nm, Φ 0.035 in H_2O), **2b** (λ_{max} 316 nm, λ_{em} 431 nm, Φ 0.03 in H_2O, a tricyclic cytosine family;[27] **3** (λ_{max} 395 nm, λ_{em} 505 nm, Φ 0.13 in H_2O), and **4**,[28−30] (λ_{max} 370 nm, λ_{em} 450 nm, Φ 0.3 in H_2O); and a tetracyclic cytosine analogue,[31,32] **5** (λ_{max} 374 nm, λ_{em} 513 nm, Φ 0.006 in 50 mM PBS containing 0.1 M sodium chloride at pH 7.4) (Figure 1).

These fluorescent nucleosides were incorporated into oligonucleotides which, in turn, were used as probes for detection of genetic material. The photophysical properties of nucleosides **1**−**5** remained the same or slightly changed upon incorporation into an oligonucleotide and after oligonucleotide hybridization.[28−30]

A great advantage of the above fluorescent pyrimidine analogues is that their size and structure enable them to be incorporated into nucleic acid with minimal disturbance of the native structure as compared to fluorescent dyes covalently linked to the backbone of the oligonucleotide.[33]

Recently, we reported on the promising properties of a novel uracil nucleoside with intrinsic fluorescence (NIF), 5-((4-methoxy-phenyl)-*trans*-vinyl)-2′-deoxy-uridine, **6** (λ_{abs} 320 nm, λ_{em} 478 nm, Φ 0.12 in H_2O)[34] (Figure 1). This fluorescent uracil analogue bears a minimal chemical modification at a position not involved in base-pairing, resulting in relatively long absorption and emission wavelengths and sufficiently high quantum yield. Analogue **6**, exhibits quantum yield that is 3000-fold larger than that of the natural uracil chromophore and maximum emission which is 170 nm red-shifted as compared to

Received: December 13, 2012

   dx.doi.org/10.1021/jm301838y | *J. Med. Chem.* XXXX, XXX, XXX−XXX

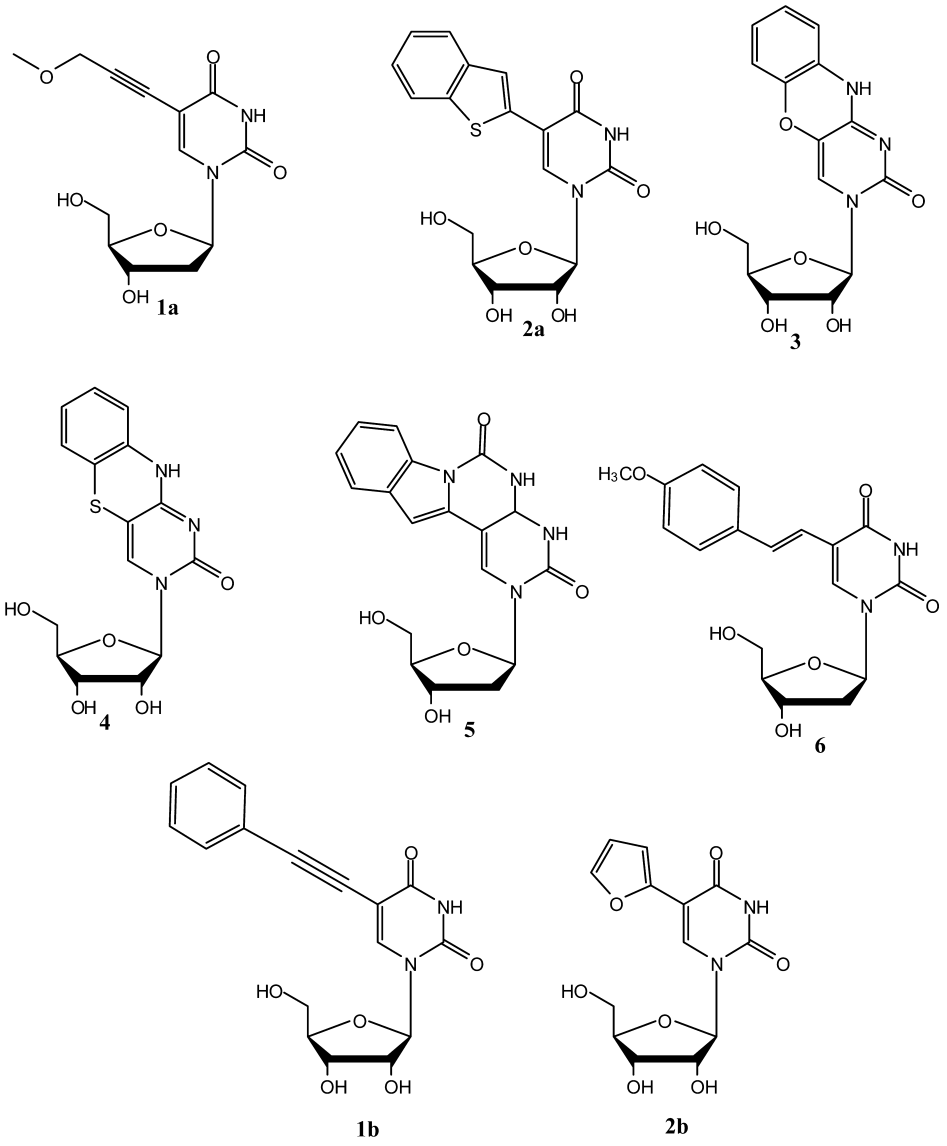

Figure 1. Previously reported fluorescent pyrimidine nucleoside analogues.

uridine. In addition, because probe **6** adopts the *anti* conformation and *S* sugar puckering, favored by B-DNA, it makes a promising nucleoside analogue to be incorporated in an oligodeoxynucleotide probe for detection of genetic material by a hybridization assay.

Here, we report labeling 15-mer oligodeoxynucleotides by one or several **6** monomers and the photophysical properties and stability of the related duplexes. We compare the fluorescence of labeled single strands to that of monomer **6** and the corresponding double strands. In addition, we analyze the dependence of photophysical properties of labeled oligodeoxynucleotides on the number of labels and the neighboring nucleobases. Finally, we demonstrate the use of monomer **6** for the preparation of a novel ds-NIF probe and for the detection of cyclin D1 breast cancer mRNA marker in total RNA extract from human cancerous cells.

RESULTS

Incorporation of 5-((4-Methoxy-phenyl)-*trans*-vinyl)-2′-deoxy-uridine, 6, into Oligodeoxynucleotides (ODNs). To develop fluorescent oligodeoxynucleotide probes for the detection of mRNA, we initially incorporated NIF analogue 5-((4-methoxy-phenyl)-*trans*-vinyl)-2′-deoxy-uridine, **6**, replacing 2′-deoxy-thymidine, into ssDNA, which is complementary to the target mRNA. The mRNA we chose to focus on was cyclin D1. The cyclin D1 protein is a major player in the control of the cell cycle.[35] The cyclin D1 gene has been convincingly implicated in oncogenesis,[36] and it is highly expressed in many cancer types and has been specifically implicated in breast cancer.[37] In addition, we also tested a unique repetitive RNA sequence called MS2[38] that is inserted into genes for the labeling of specific mRNAs.[39] Because of the repetitive nature of the sequence, it is possible to obtain a strong signal via the binding of several identical probes to the sequence repeats.

We first prepared the protected and activated nucleoside phosphoramidite, **10**, starting from 5-I-2′-deoxy-uridine, **7**. Thus, 5-iodo-2′-deoxyuridine, **2**, was protected with 4,4′-dimethoxytrityl group at C5′-OH, to obtain **8** in 85% yield, which was then employed as a substrate in a Suzuki coupling reaction with *trans*-2-(4-methoxy-phenyl)-vinyl boronic acid to give **9** in 86% yield. Finally, 5′-DMTO-3′-O phosphoramidite,

dx.doi.org/10.1021/jm301838y | J. Med. Chem. XXXX, XXX, XXX−XXX

Scheme 1. Synthesis of Phosphoramidite 10[a]

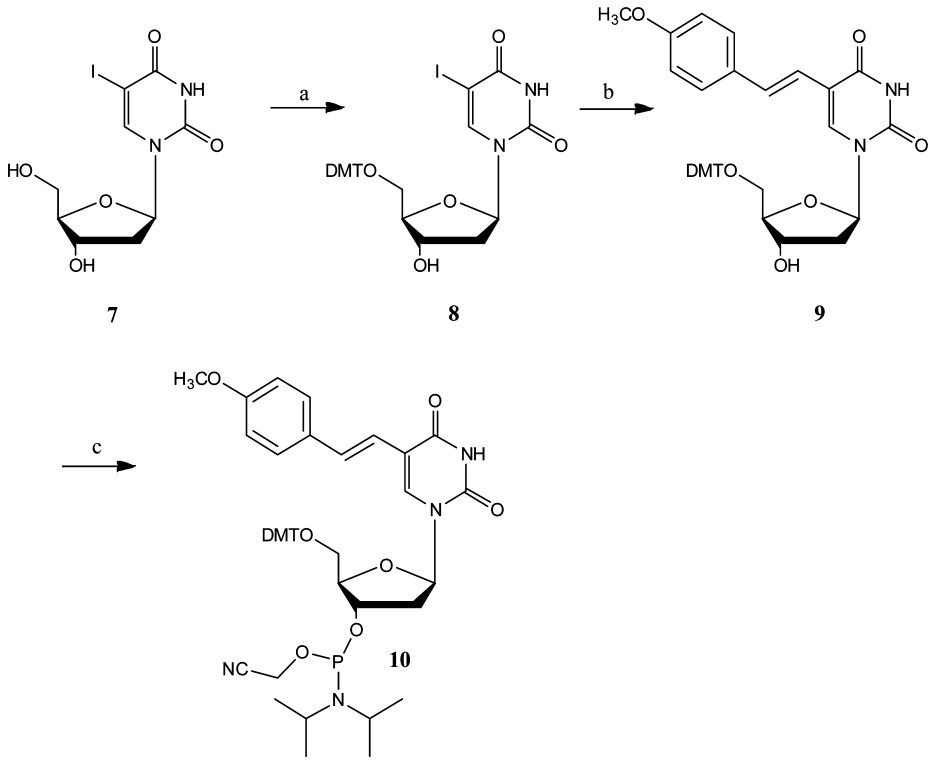

[a]Reaction conditions: (a) 4,4′-dimethoxytrityl chloride (1.2 equiv), pyridine, 80% yield; (b) *trans*-2-((4-methoxy)-phenyl) boronic acid (1.25 equiv), Na_2CO_3 (3 equiv), TPPTS (0.25 equiv), $Pd(OAc)_2$ (0.05 equiv), CH_3CN:H_2O (2:1), 86% yield; (c) *N*,*N*′-diisopropylcyanoethyl-phosphoramidite chloride, TEA, CH_2Cl_2, 75% yield.

Table 1. Photophysical Properties of Labeled MS2-Derived ODNs (1, 3, 5, 7, 9, 11) and Their Corresponding Duplexes (2, 4, 6, 8, 10, 12) in PBS Buffer[a]

entry	DNA sequence (MS2-ODN)	λ_{abs} max (nm)	λ_{em} max (nm)	Φ	T_m (°C)
unmodified duplex (control)	3′-ATCCTAGATTACTTG-5′	260			43
	5′-TAGGATCTAATGAAC-3′				
1	3′-A**U**CCTAGATTACTTG-5′	331	461	0.020	
2	3′-A**U**CCTAGATTACTTG-5′	330	460	0.025	49
	5′-TAGGATCTAATGAAC-3′				
3	3′-A**U**CCTAGATTACTTG-5′	331	463	0.018	
4	3′-A**U**CCTAGATTACTTG-5′	333	456	0.023	45
	5′-TAGGATCTAATGAAC-3′				
5	3′-ATCCTAGA**U**TACTTG-5′	334	459	0.013	
6	3′-ATCCTAGA**U**TACTTG-5′	334	455	0.023	64
	5′-TAGGATCTAATGAAC-3′				
7	3′-ATCCTAGAT**U**ACTTG-5′	334	463	0.009	
8	3′-ATCCTAGAT**U**ACTTG-5′	334	459	0.029	59
	5′-TAGGATCTAATGAAC-3′				
9	3′-ATCCTAGATTAC**U**TG-5′	332	462	0.150	
10	3′-ATCCTAGATTAC**U**TG-5′	329	489	0.013	46
	5′-TAGGATCTAATGAAC-3′				
11	3′-AUCC**U**AGA**U**UACTTG-5′	328	462	0.008	
12	3′-AUCC**U**AGA**U**UACTTG-5′	325	459	0.014	60
	5′-TAGGATCTAATGAAC-3′				

[a]T_m values are given for all duplexes. Bold U denotes fluorescent deoxyuridine label.

10, was prepared upon treatment of **9** with phosphoramidite chloride to obtain compound **10** in 75% yield (Scheme 1).

Phosphoramidite, **10**, was used as a monomer for the preparation of 15-mer oligodeoxynucleotides (ODNs) which contain a single label or multilabels replacing T at different positions of the oligonucleotide sequence. Two series of labeled 15-mer deoxyoligonucleotides were prepared: (1) ODNs derived from MS2[40,41] bacteriophage RNA sequence (Table 1) and (2) ODNs derived from cyclin D1[42] mRNA sequence (Table 2). We chose a 15-mer long oligonucleotide because 15-

dx.doi.org/10.1021/jm301838y | J. Med. Chem. XXXX, XXX, XXX−XXX

Table 2. Photophysical Properties of Labeled Cyclin D1-Derived ODNs (13, 15, 17, 19, 21, 23, 25, 27, 29) and Their Corresponding Duplexes (14, 16, 18, 20, 22, 24, 26, 28, 30) in PBS Buffer[a]

entry	DNA sequence (cyclin D1-ODN)	λ_{abs} max (nm)	λ_{em} max (nm)	Φ	T_m (°C)
unmodified duplex (control)	3′-CTTGTTCGAGTTCAC-5′	260			49
	5′-GAACAAGCTCAAGTG-3′				
13	3-C**U**TGTTCGAGTTCAC-5′	327	459	0.034	
14	3′-C**U**CTTCGAGTTCAC-5′	324	455	0.090	50
	5′-GAACAAGCTCAAGTG-3′				
15	3′-CT**U**GTTCGAGTTCAC-5′	327	460	0.040	
16	3′-CT**U**GTTCGAGTTCAC-5′	327	455	0.080	36
	5′-GAACAAGCTCAAGTG-3′				
17	3′-CTTGUTCGAGTTCAC-5′	327	457	0.050	
18	3′-CTTGUTCGAGTTCAC-5′	327	453	0.140	41
	5′-GAACAAGCTCAAGTG-3′				
19	3′-CTTGUTCGAGTTCAC-5′	327	466	0.110	
20	3′-CTTGT**U**CGAGTTCAC-5′	326	452	0.300	55
	5′-GAACAAGCTCAAGTG-3′				
21	3′-CTTGTTCGAG**U**TCAC-5′	327	458	0.100	
22	3′-CTTGTTCGAG**U**TCAC-5′	327	447	0.250	45
	5′-GAACAAGCTCAAGTG-3′				
23	3′-CTTGTTCGAGT**U**CAC-5′	329	460	0.060	
24	3′-CTTGTTCGAGT**U**CAC-5′	327	448	0.260	50
	5′-GAACAAGCTCAAGTG-3′				
25	3′-C**U**TGTTCGAGT**U**CAC-5′	328	463	0.130	
26	3′-C**U**TGTTCGAGT**U**CAC-5′	328	453	0.020	51
	5′-GAACAAGCTCAAGTG-3′				
27	3′-C**U**TGT**U**CGAGT**U**CAC-5′	328	460	0.150	
28	3′-C**U**TGT**U**CGAGT**U**CAC-5′	328	457	0.016	50
	5′-GAACAAGCTCAAGTG-3′				
29	3′-C**U**UG**U**UCGAG**U**UCAC-5′	325	459	0.005	
30	3′-C**U**UG**U**UCGAG**U**UCAC-5′	325	458	0.004	47
	5′-GAACAAGCTCAAGTG-3′				

[a] T_m values are given for all duplexes.

mer is the minimal length which would ensure specific binding to target MS2 or cyclin D1 sequences.

ODNs containing the modified uridine monomer(s) were prepared on solid-phase according to conventional DNA synthesis protocol. The coupling yields were always higher than 95%. Deprotection of the oligomers was performed with aqueous 33% NH_4OH at 37 °C over 24 h. Purification of the oligonucleotides was achieved on Poly-Pak II column. The oligonucleotides were detritylated with 2% TFA, and further purification was performed by reversed-phase HPLC. The purified oligomers were characterized by MALDI-TOF mass spectrometry.

Because emission of fluorescent nucleosides within oligonucleotides is sensitive to neighboring nucleobases,[27,31] we incorporated nucleoside **6** at various positions of the studied 15-mer oligonucleotides while keeping all the other bases the same. In addition, differently multilabeled oligonucleotides were tested.

ODN labeling included: (1) MS2 derived ODNs labeled at positions 2 or 5 or 9 or 10 or 13, and tetra-labeled at 2, 5, 9, and 10 (Table 1), and (2) cyclin D1 ODNs derived labeled at positions 2 or 3 or 5 or 6 or 11 or 12, dilabeled at positions 2 and 6, or 2 and 12, trilabeled at positions 2, 6, and 12, and hexa-labeled at positions 2, 3, 5, 6, 11, and 12 (Table 2).

These series of oligomers were used to explore whether our monomer of choice, **6**, when incorporated into a ss-ODN, would trigger a significant quantum yield change upon duplex formation.

Photophysical Characterization of MS2-Derived Labeled ODNs 1−12. In the MS2-derived ODN series (entries **1−12**, Table 1), six labeled single-strand oligonucleotides were synthesized. For every oligomer, the corresponding duplex was prepared. All studied ODNs, either single- or double-strand, were excited at 325−334 nm and emitted at 455−463 nm, except for the double strand labeled at position 13, which emitted at 489 nm. The position 4-labeled ODN (entry **11**), exhibited a very low Φ value of 0.008, however this value increased 2-fold upon duplex formation (entry **12**). The quantum yield also increased 3-fold in monolabeled ODN at position 10 (entry **7**) upon duplex formation (entry **8**). The Φ value of three monolabeled ODNs at position 2, 5, or 9 (entries **1**, **3**, and **5**) remained unchanged upon duplex formation (entry **2**, **4**, and **6**). The ODN monolabeled at 13 position displayed an exceptionally large 11.5-fold reduction of quantum yield upon duplex formation, changing from 0.15 (entry **9**) to 0.013 (entry **10**).

Photophysical Characterization of Cyclin D1-Derived Labeled ODNs 13−30. In the series of cyclin-D1 derived ODNs (entries **13−30**), nine labeled single-stranded oligonucleotides were synthesized. For every oligomer, the corresponding duplex was prepared (Table 2).

All studied ODNs, either single- or double-strand, were excited at 325−329 nm and emitted at 447−460 nm (Figure 2).

dx.doi.org/10.1021/jm301838y | J. Med. Chem. XXXX, XXX, XXX−XXX

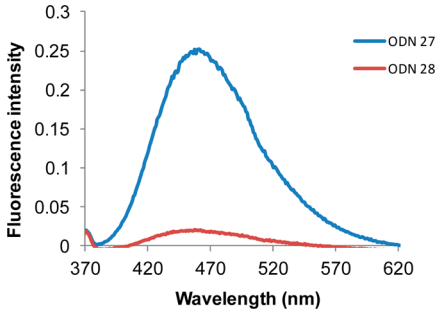

Figure 2. Emission spectra of ODN **27** (ssDNA) vs **28** (dsDNA).

Six monolabeled fluorescent ssODNs (entries **13**–**23**) exhibited Φ values of 0.034–0.11, however, these values increased 2–4-fold upon duplex formation (entries **14**–**24**). Yet, the hexa-labeled ODN retained its fluorescent quantum yield value upon duplex formation (entries **19** and **29**). The Φ value of dilabeled and trilabeled ODN (entry **25**, Φ 0.13), and entry **27**, Φ 0.15) decreased by a factor of 6.5 and 9.5, respectively.

Circular Dichroism Measurements of Duplexes of Cyclin D1-Derived ODNs 16–30. We used CD spectroscopy to analyze the secondary structure of duplexes containing 5-((4-methoxy-phenyl)-*trans*-vinyl)-2′-deoxy-uridine, Figure 3). The

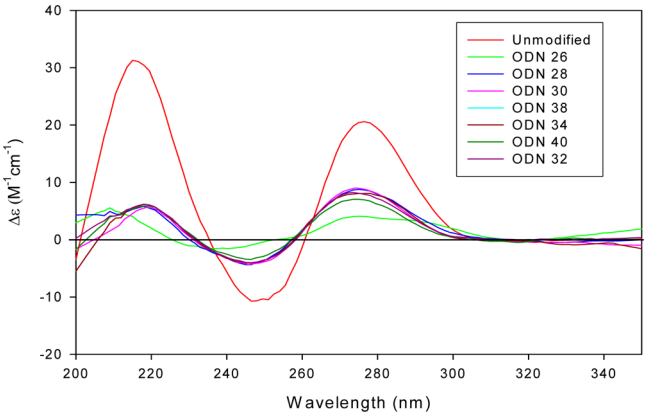

Figure 3. CD spectra of cyclin-D1 derived ODN duplexes, **16**–**30**.

CD spectra exhibit positive bands at 271 and 220 nm as well as a negative band at 245 nm. The general appearance of the CD signal between 300 and 200 nm resembles that of a common right-handed helical B-DNA conformation, which is normally characterized by a positive band centered at 275 nm, a negative band at 240 nm, and a band which could be positive or negative at 220 nm.[43]

Thermostability of Duplexes. The feasibility of the use of the above ODNs for detection of genetic material depends on the thermostability of the related duplexes.

The T_m values of almost all hybrids of our new fluorescent ODNs with the complementary DNA strands are 45–61 °C, indicating that they are thermally stable (Tables 1, 2). In all MS2-derived sequences, T_m values were increased by 6–21 °C as compared to the corresponding parent duplex (control). In cyclin D1, six sequences showed an increase in T_m of 1–6 °C (entries **14**, **20**, **24**, **26**, and **28**) whereas four sequences showed a 2–10 °C decrease (entries **16**, **18**, **22**, and **30**).

Proving the Applicability of ds-NIF Probe for Detection of Target ssDNA. To prove the applicability of 5-((4-methoxy-phenyl)-*trans*-vinyl)-2′-deoxy-uridine, **6**, labeled ODNs for detection of ssDNA, we selected an ODN exhibiting a large change of fluorescence upon hybridization/dehybridization. Specifically, we selected a cyclin D1-derived ODN labeled at positions 2, 6, and 12 (entry **27**), the fluorescence of which is reduced 9.5-fold upon duplex formation (Figure 2). Furthermore, we devised a NIF-duplex probe composed of a 15-mer ODN (entry **28**):35-mer duplex (Figure 4). This ds probe

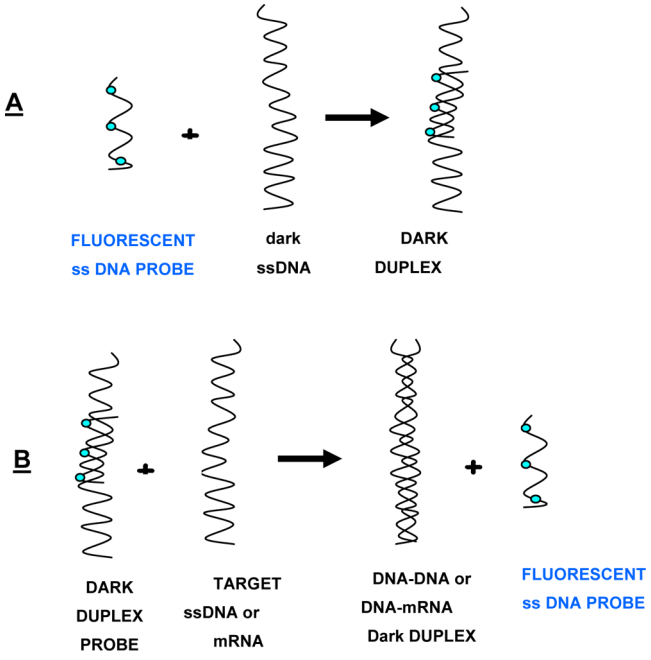

Figure 4. ds-NIF probe methodology for detection of ssDNA or mRNA. (A) Preparation of ds-NIF probe from fluorescent ss-DNA and a longer complementary ssDNA. (B) Application of ds-NIF probe for the detection of target ssDNA/mRNA.

(Figure 4A) is relatively dark. When this ds-NIF probe is added to target ssDNA or mRNA, it undergoes dehybridization and concomitant by rehybridization with the target, with release of the fluorescent NIF-ssODN (Figure 4B). In this way, the ds-NIF probe indicates the presence of the target ssDNA or mRNA.

Specifically, we hybridized ODN **27** (Φ 0.15) with a 35-mer ODN, the middle part of which is complementary to ODN **27**, to obtain double-stranded DNA, **28** (Φ 0.06). To this duplex we added at room temperature another 35-mer ODN (5 equiv), representing target DNA, which is complementary to the first mentioned 35-mer. At this point, we observed a time-dependent increase in fluorescence intensity, indicating the release of the fluorescent 15-mer ODN and a concomitant formation of a 35:35-mer duplex (Figure 5). In this way, we achieved a significant signal:background ratio (13:1), indicating clearly the presence of target oligonucleotide.

In addition, we validated the ds-NIF probe methodology by monitoring the dehybridization–rehybridization process and concomitant release of the fluorescent probe **27** by gel electrophoresis (Figure 6). The gel picture depicts 7 lanes:

In lane 1: 15-mer fluorescent ODN **27**. Lanes 2 and 3: 35-mer ODNs complementary to each other. Lane 4: 15-mer ODN **27**:35-mer duplex (blue arrow). Lane 5: 35-mer:35-mer ds. Lane 6: 15-mer:15-mer duplex. Lane 7: 15-mer:35-mer duplex upon addition of complementary 35-mer ODN. Clearly,

dx.doi.org/10.1021/jm301838y | J. Med. Chem. XXXX, XXX, XXX–XXX

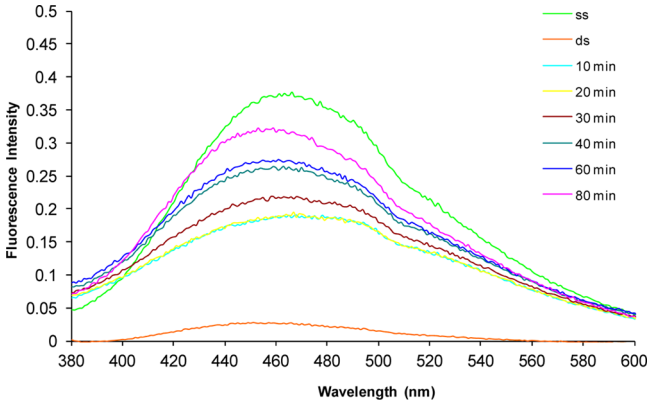

Figure 5. Time-dependent fluorescence of 50 μM ds-NIF probe in the presence of target ssDNA in PBS buffer.

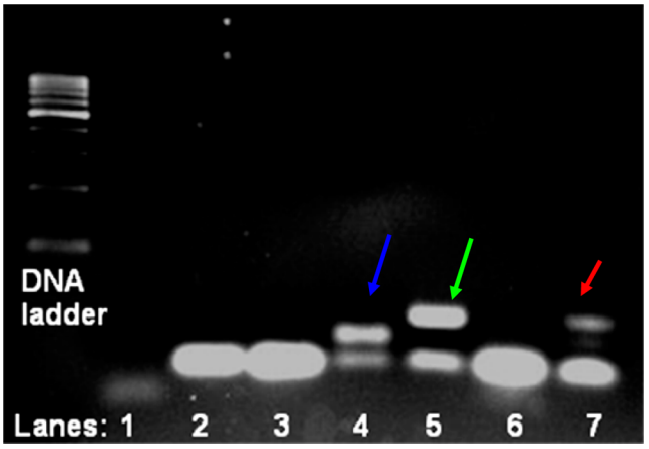

Figure 6. Gel electrophoresis monitoring of ds-NIF probe methodology for the detection of target ssDNA visualized by ethidium bromide.

the band of 15-mer:35-mer duplex weakened (red arrow) and the band of 35-mer:35-mer ds became stronger (green arrow), indicating dehybridization of 15-mer:35-mer duplex and rehybridization to obtain 35-mer:35-mer ds. Indeed, these data support the occurrence of the mechanism of the ds-NIF probe methodology as observed by fluorescence monitoring (Figure 5).

In conclusion, upon addition of complementary 35-mer single-strand to double-stranded DNA, **28**, 15:35-mer, we observed an increase in fluorescence intensity, indicating the release of the fluorescent 15-mer single-strand and formation of a 35:35-mer duplex. The reason for this rehybridization is probably formation of a more stable duplex (35:35-mer) than duplex **28** (15:35-mer).

Proving the Applicability of ds-NIF Probe for Detection of Cyclin D1 in RNA Cell Extracts. Next, we proved the ds-NIF probe methodology by monitoring the fluorescence intensity of probe **28** in RNA extracted from the human U2OS osteosarcoma cell line (Figure 7). The ds-NIF probe was added to total cell RNA extracts containing high levels of cyclin D1 from a cell line stably overexpressing a cyclin D1 gene, 1842 ng/μL.

In addition, probe **28** was added to extracts of cells expressing basal levels of cyclin D1 found in U2OS cells. Fluorescent ssODN **27** was used as a positive control, while ds-NIF probe, **28**, was the negative control. Additional controls

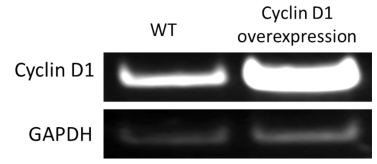

Figure 7. Levels of cyclin D1 mRNA expression were three times higher in U2OS cells overexpressing GFP-cyclin D1 than in wild-type U2OS cells (WT), as measured by quantitative RT-PCR. Glyceraldehyde-3-phosphate dehydrogenase (GAPDH) mRNA levels were used as a control.

were the RNA extract alone and RNA extract with MS2 ODN probe, **10**. Upon addition of the probe to RNA extract containing high levels of cyclin D1, we observed a time-dependent increase in fluorescence intensity up to 3-fold vs the ds-NIF probe fluorescence after 90 min (signal:background ratio 3:1). This fluorescent enhancement indicates the release of the fluorescent 15-mer ODN, **27**, and the formation of a DNA:cyclin D1 RNA duplex (Figure 8).

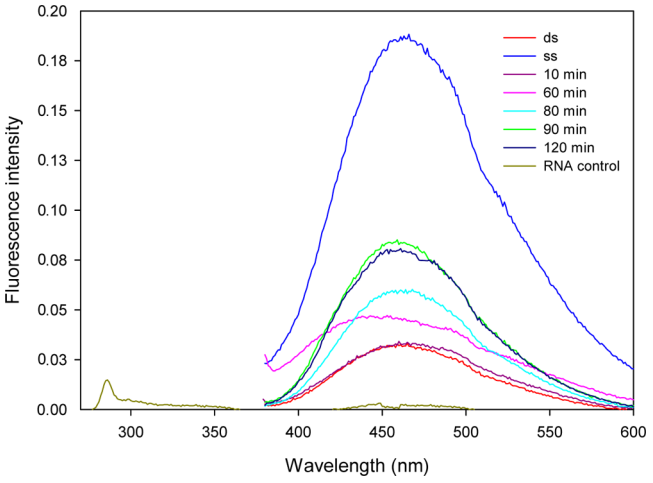

Figure 8. Time-dependent fluorescence of 50 μM ds-NIF/ssNIF probes, **28**/**27** in PBS buffer, in the presence of RNA cell extract containing high levels of cyclin D1.

Yet, addition of ODN **28** to the RNA extract of cells expressing basal levels of cyclin D1 did not result in any increase of fluorescence intensity (Supporting Information p S1).

Furthermore, addition of the MS2-based probe, ODN **10**, to the RNA extract of cells expressing high levels of cyclin D1, did not result in any elevation of intensity (Supporting Information p S2).

In this way we demonstrated qualitatively the efficiency of the ds-NIF probe method for the detection of breast cancer marker, cyclin D1, in RNA extracted from cancerous cells.

DISCUSSION

Selection of ODNs for Validation of the ds-NIF Probe Methodology. To validate the proposed ds-NIF probe method, we first examined a NIF probe containing monomer **6** on an existing gene system expressing mRNA containing MS2 24 sequence repeats[44] which may result in amplification of the mRNA signal. Hence, the binding of up to 24 probe molecules to each mRNA molecule is expected. MS2 is a mRNA, but we studied its DNA variant because of its higher

dx.doi.org/10.1021/jm301838y | J. Med. Chem. XXXX, XXX, XXX−XXX

stability. Next, we applied our methodology to the detection of cyclin D1, a mRNA marker of breast cancer.[45] We selected a 15-mer ODN from the cyclin D1 mRNA sequence, which is specific to this mRNA only and does not appear in any other endogenous mRNA. This 15-mer ODN was selected by Basic Local Alignment Search Tool (BLAST) and has six bases of adenine which are complementary to the fluorescent thymidine-like monomer **6**.

The Fluorescence of Monomer 6 is Quenched upon its Incorporation into Monolabeled MS2 and Cyclin D1 ssODNs. Monolabeled MS2 ODNs (entries **1**, **3**, **5**, and **7**) showed a decreased quantum yield as compared to that of monomer **6** up to 13-fold. In those monolabeled ODNs, one of monomer **6** neighboring nucleobases was adenine. Likewise, monolabeled cyclin D1 ODNs (entries **13**, **15**, **17**, and **23**) exhibited fluorescence quenching as compared to Φ value of monomer **6** itself. In those monolabeled ODNs, one of monomer **6** neighboring nucleobases was thymine. Yet, when the neighboring nucleobases were C or G (entries 9, 19, and 21), the quantum yield remained high (Φ 0.1−0.15) as for monomer **6** itself.

Fluorescence is Quenched Dramatically when Two Adjacent Labels are Introduced to Cyclin D1 and MS2 ODNs. The fluorescence of ss-cyclin D1 hexa-labeled ODN (entry **29**) and MS2 tetra-labeled ODN (entry **11**) was quenched dramatically compared to that of monomer **6**. In these two oligomers, there were two adjacent monomers **6**. The close proximity between two monomers **6** may possibly cause collisions in the excited state.[46] Following this event, energy may possibly be emitted as heat and not as a photon emission, which may result in quenching.

Cyclin D1 Multilabeled ODNs Showed Decreased Φ Value upon Duplex Formation. In cases of di- and trilabeled ss ODNs (entries **25** and **27**, respectively), Φ value was decreased upon duplex formation (entries **26** and **28**). Possibly, intramolecular interactions between the labels in the duplex form might be the cause for this phenomenon, although quenching by water molecules might also contribute to the overall fluorescence quenching. It is also notable that even in the ss-DNA, addition of multiple labels tends to decrease Φ, as exemplified by ODN **29** that bears six labels and shows a negligible quantum yield of 0.005.

CD Spectra of Labeled DNA Sequences Reveal Features Characteristic of B-DNA. Circular dichroism measurements of the series of labeled ds-ODNs sequences (entries **2**−**40**), where neighboring bases of monomer **6** vary, all resemble B-DNA form. Thus, monomer **6** does not seem to distort the duplex conformation (Figure 3).

Incorporation of Monomer 6 in ODNs Usually Increases the Stability of the Resulting Duplexes. Development of a fluorescent probe, the application of which is based on hybridization, requires not only suitable photophysical properties in ss- and ds-DNA but also duplex stability. In all MS2-derived labeled duplexes, T_m increased on the average by 10.8 °C as compared to the unmodified duplex. In cyclin D1-derived labeled duplexes, T_m increased on the average by 2.5 °C as compared to that of the unmodified duplex. The increased stability of these duplexes may indicate favorable stacking interactions of monomer **6** as compared to those of T itself with its neighboring nucleobases.

Thermal Stability (T_m) is Highly Sensitive to Neighboring Bases of Monomer 6. In both MS2 and cyclin-D1 derived ODN duplexes series, we observed a clear dependence of T_m on the bases adjacent to the NIF monomer, **6**.

In the MS2 series, the presence of an A and a C on either side of **6** results in a modest increase in T_m (ΔT_m = +2 °C for A**U***C and ΔT_m = +6 °C for C**U***A, entries **11** and **13** in Table 2, respectively). However, changing C to T results in a dramatic increase in T_m: ΔT_m = +21 °C for A**U***T and ΔT_m = +16 °C for T**U***A (entries **15** and **17** in Table 2, respectively). In fact, this is quite a remarkable increase in T_m for a single substitution.

Interestingly, we have also observed a correlation between ΔT_m and Φ values. Namely, Φ is slightly increased for the A**U***C and C**U***A ODNs upon duplex formation, whereas Φ is doubled and even tripled for the A**U***T and T**U***A ODNs (ΔT_m = +16 °C to +21 °C). It is possible that increased thermal stability reduces the accessibility of water molecules to the NIF probe, **6**, resulting in less quenching and, as a consequence, higher Φ values.

In the cyclin D1-derived ODNs series, we also noticed the effect of neighboring bases on T_m, although the effect is less pronounced.

Thus, having a C and a T as neighboring bases results in a modest increase in T_m: C**U***T (entry **13**, Table 2) ΔT_m = +1 °C and T**U***C (entries **19** and **23**, Table 2) result in ΔT_m = +6 °C and +1 °C, respectively. Replacing C with G leads to a significant decrease in thermal stability where T**U***G (entry **15**, Table 2) and G**U***T (entries **17** and **21**, Table 2) exhibit a ΔT_m −10 °C ΔT_m's values of −8 °C and −4 °C, respectively.

Application of the ds-NIF Probe Methodology for the Detection of Cyclin D1 mRNA. The limitations of current standard practice for the diagnosis of DNA or RNA emphasize the urgent need for conceptually different fluorescent probes.[47,48]

Therefore, we demonstrated here the ability of ds-NIF probe methodology to detect cyclin D1 mRNA in cancerous cell extract. This methodology is centered on nucleoside with intrinsic fluorescence, monomer **6**, which is incorporated into oligodeoxynucleotides that subsequently hybridize to form ds-NIF probe probes. This methodology may be applied in those cases where the ss-NIF-DNA probes exhibit significantly different photophysical properties than those of ds-DNA (RNA):NIF-DNA. The unique photophysical properties and T_m values of DNA:NIF-DNA vs mRNA:DNA duplexes may be harnessed to detect target mRNA (Figure 4).

The ds-NIF probe method demonstrated here involves the preparation of a duplex of NIF-DNA and a longer complementary DNA, the duplex is termed NIF probe, which is the actual probe. This ds-NIF probe is relatively dark, i.e., has a low Φ value (Figure 4A). Next, this probe is allowed to interact with the target mRNA, resulting in the formation of DNA:mRNA duplex and the release of the fluorescent ss-NIF-DNA, thus indicating the presence of the target mRNA (Figure 4B).

We found that the fluorescence of the NIF analogue **6** was quenched in most cases upon incorporation into a single-strand ODN, up to 24-fold. Yet, fluorescence quantum yield of the related duplexes increased, decreased, or remained unchanged as compared to the corresponding labeled-ss-ODNs. On the basis of the 9.5-fold reduction of fluorescence upon duplex formation with cyclin D1 derived ODN **27** (Table 2), we designed a NIF probe consisting of a duplex of ODN **27** with a longer complementary strand for the detection of cyclin D1 mRNA in the presence of a ss-DNA variant of cyclin D1 mRNA

dx.doi.org/10.1021/jm301838y | J. Med. Chem. XXXX, XXX, XXX−XXX

(probe **28**). Indeed, when tested, this duplex dehybridized and released the significantly more fluorescent ODN **27** within 80 min at room temperature, thus indicating the presence of target oligonucleotide.

The ds-NIF-DNA Probe Methodology Is Useful for Detection of Cyclin D1 mRNA in Cancerous Cell total RNA Extract. The above ds-NIF-DNA probe, **28**, underwent dehybridization in cell RNA extracts containing high levels of cyclin D1 mRNA and released the significantly more fluorescent ODN **27** within 90 min at room temperature, thus indicating the presence of target cyclin D1. Furthermore, the fluorescence intensity of this probe remained unchanged in the presence of low levels of cyclin D1 in the extract. In addition, the fluorescence intensity did not increase upon addition of a MS2 ds-NIF probe into the RNA extract containing high levels of cyclin D1. The results confirm the usefulness of ds-NIF probe methodology for the diagnosis of breast cancer subtype by using extracts of biopsies.

CONCLUSIONS

In summary, we propose a novel probe for the efficient detection of cyclin D1 mRNA in a total RNA cell extract. This new methodology may have several benefits over current procedures. For instance, synthetic procedures currently performed on the genetic material in the biological sample prior to detection may be circumvented. Instead, ready-made fluorescent nucleosides may be used for automatic synthesis of the probe. In addition, no toxic or water insoluble fluorescent dyes are used. Furthermore, background fluorescence of unreacted probe is not significant, which may be especially useful when working with cells. The suitability of the new methodology for additional applications will be reported in due course.

EXPERIMENTAL SECTION

General. Compounds were characterized by nuclear magnetic resonance using Bruker AC-200, DPX-300, or DMX-600 spectrometers. ^{1}H NMR spectra were measured at 200, 300, or 600 MHz. Phosphoramidite monomer was characterized also by ^{31}P NMR in CD_3CN, using 85% aq H_3PO_4 as an external reference on Bruker AC-200. Chemical shifts are expressed in ppm. Nucleosides were analyzed under ESI (electron spray ionization) conditions on a Q-TOF microinstrument (Waters, UK). MALDI-TOF mass spectra of oligonucleotides were measured with a mass spectrometer in a negative ion mode with HPA matrix. Progress of reactions was monitored by TLC on precoated Merck silica gel plates (60F-254). Visualization was accomplished by UV light. Medium pressure chromatography was carried out using automated flash purification system (Biotage SP1 separation system, Uppsala, Sweden). All moisture sensitive reactions were carried out in flame-dried reaction flasks with rubber septa, and the reagents were introduced with a syringe. All reactants in moisture sensitive reactions were dried overnight in a vacuum oven. Absorption spectra were measured on a UV-2401PC UV−vis recording spectrophotometer (Shimadzu, Kyoto, Japan). Emission spectra were measured using Aminco-Bowman series 2 (AB2) luminescence spectrometer (Thermo Electron Corporation, Markham, Ontario, Canada). Absorption and fluorescence spectra were recorded in PBS buffer containing 100 mM NaCl and 10 mM phosphate. Primary oligonucleotides synthesis was carried out on an ABI DNA/RNA synthesizer (Forster City, USA) on a 1 μmol scale by standard automated solid-phase method using natural β-cyanoethyl-phophoramidite bases. Cleavage from the solid support and deprotection were carried out in 33% NH_4OH at 37 °C for 24 h. Purification of oligonucleotides was achieved on a Poly-Pak II column (Glen Research, Sterling, VA). Final purification of oligonucleotides was achieved on an HPLC (Merck−Hitachi) system, using an analytical reverse-phase column (Gemini 5μ C-18 110A, 150 mm × 4.6 mm, 5 μm, Phenomenex, Torrance, CA, USA) in 0.1 M TEAA buffer: CH_3CN 97:3 to 75:25 in 30 min (1 mL/min). Purity was determined by analytical HPLC and confirmed >95% pure. Thermal denaturation curves measurements were performed on a Cary 300 spectrophotometer (Varian Inc.). The extinction coefficients for the modified oligonucleotides were approximated by the linear combination of the extinction coefficients of the natural nucleotides and the extinction coefficient of the modified nucleoside. To account the base stacking interactions, this linear combination was multiplied by 0.9 to give the final extinction coefficients for the oligomers. The individual extinction coefficients at 260 nm used were ε_T = 8400 M^{-1} cm^{-1}, ε_C = 7050 M^{-1} cm^{-1}, ε_G = 12 010 M^{-1} cm^{-1}, ε_A = 15 200 M^{-1} cm^{-1}, and $\varepsilon_{\text{modified U}}$ = 13 500 M^{-1} cm^{-1}.

Synthesis. *1-(5-((Bis(4-methoxyphenyl)(phenyl)methoxy)-methyl)-4 hydroxytetrahydrofuran-2-yl)-5-iodopyrimidine-2,4-(1H,3H)-dione,* ***8****.* Compound 7 (2 g, 5.65 mmol) was dissolved in dry pyridine (29 mL). The pyridine was evaporated to half volume. DMT-Cl (2.3 g, 6.78 mmol) was added, and the orange solution was stirred for 19 h under nitrogen atmosphere at RT. After 19 h, a new spot was observed on TLC (98:2 CH_2Cl_2:MeOH). Cold water (80 mL) was added to the orange solution, and the mixture was extracted twice with CH_2Cl_2 (2 × 100 mL). The two organic phases were combined and dried over Na_2SO_4. The solvent was evaporated, and the product was purified on a silica gel column (98:2 CH_2Cl_2:MeOH) to yield compound **8** as a white solid in 84% (3.14 g). ^{1}H NMR (300 MHz, CD_3CN): δ 8.00 (s, 1H) 7.37−6.86 (m, 13H), 6.13(t, J = 3.5 Hz, 1H), 4.42−4.40 (m, 1H), 3.96−3.94 (m, 1H), 3.76 (s, 6H), 3.4−3.25 (m, 2H), 1.94 (m, 2H). ^{13}C NMR (300 MHz, $CDCl_3$) δ 127.88, 128.15, 129.25, 135.52, 135.64, 144.50, 144.60, 150.52, 158.65, 160.7, 127.09, 113.46, 113.19, 87.00, 86.77, 85.89, 77.68, 77.26, 76.83, 72.42, 69.02, 65.89, 63.74, 55.34, 41.43, 15.311 ppm. λ_{max} (CH_3CN) = 278 nm ESI+ MS m/z: ($C_{30}H_{29}IN_2O_7$) 679 (MNa^+). Anal. Calcd for $C_{30}H_{29}IN_2O_7$: C, 30.18; H, 4.22; I, 35.44; N, 7.82; O, 22.34. Found: C 29.88, H 4.02, I, 35.24; N 8.05, O 22.81.

(E)-1-(5-((Bis(4-methoxyphenyl)(phenyl)methoxy)methyl)-4 hydroxytetrahydrofuran-2-yl)-5-(4-methoxystyryl)pyrimidine-2,4-(1H,3H)-dione, ***9****.* Water−acetonitrile (6: 3 mL) was added through a septum to nitrogen-purged round-bottom flask containing **8** (1 g, 1.523 mmol), *trans*-2-(4-methoxy-phenyl)-vinylboronic acid (338.86 mg, 1.9 mmol), $Pd(OAc)_2$ (17.24 mg, 0.076 mmol), TPPTS (216.42 mg, 0.38 mmol), and Na_2CO_3 (480 mg, 4.56 mmol). The mixture was stirred under reflux for 4 h. A new spot was observed on TLC (9:1 $CHCl_3$: MeOH) while starting material disappeared. Acetonitrile was removed, water was added and the crude residue was freeze-dried. The product was purified on a silica gel column (90:10 $CHCl_3$:MeOH), yielding compound **9** in 88.5% (893 mg) as a white solid. ^{1}H NMR (300 MHz, CD_3CN): δ 7.80 (s, 1H) 7.48−6.72 (m, 11H), 7.21−6.98 (m, 8H), 6.31−6.26 (m, 2H), 4.52 (m, 1H), 4.00 (m, 1H), 3.99 (s, 3H), 3.75 (s, 6H), 3.49−3.15 (m, 2H) ppm. ^{13}C NMR (300 MHz, $CDCl_3$) δ 40.14, 40.29, 40.57, 40.84, 55.41, 55.52, 55.58, 64.23, 70.87, 84.88, 86.23, 111.88, 113.7, 114.44, 119.31, 127.27, 127.62, 128.21, 128.36, 128.47, 130.11, 130.24, 130.41, 136.01, 137.55, 145.18, 149.89, 158.59, 159.171, 162.63 ppm. λ_{max} (CH_3CN) = 327 nm. ESI+ MS m/z: ($C_{39}H_{38}N_2O_8$) 685 (MNa^+). Anal. Calcd for $C_{39}H_{38}N_2O_8$: C, 59.33; H, 6.64; N, 7.69; O, 26.34. Found: C, 59.61; H, 6.39; N, 7.54; O, 26.46.

(E)-2-((Bis(4-methoxyphenyl)(phenyl)methoxy)methyl)-5-(5-(4-methoxystyryl) 2,4-Dioxo-3,4-dihydropyrimidin-1(2H)-yl)-tetrahydrofuran-3-yl cyanomethyldiisopropylphosphoramidite, ***10****.* Nucleoside **9** (200 mg, 0.3 mmol) was dissolved in CH_2Cl_2 (3 mL) in a flame-dried two-neck flask under N_2. Diisopropylethylamine (0.54 mmol, 0.13 mL) and phosphoramidite chloride (83.65 μL, 1.25 equiv) were added to this solution. The clear yellow solution was stirred at RT for 19 h. The solvent was evaporated, and the crude residue was immediately separated on a silica gel column using hexane:EtOAc (2:8) as an eluent containing 3% TEA. Compound **10** was obtained in 78% yield (200 mg) as yellow oil. ^{1}H NMR (200 MHz, CD_3CN): δ 7.83 (s, 1H) 7.51−7.22 (m, 11H), 6.95−6.67 (m, 8H), 6.3−6.25 (m, 2H), 4.81−4.55(m, 1H), 4.07−4.04 (m, 1H), 3.66 (s, 3H), 3.61 (s,

dx.doi.org/10.1021/jm301838y | J. Med. Chem. XXXX, XXX, XXX−XXX

6H), 3.59−3.56 (m, 4H), 2.50−2.47 (m, 4H) ppm. ^{31}P NMR (CD_3CN): δ 148.54 ppm. ESI+ MS m/z: ($C_{48}H_{55}N_4O_9P$) 862 (MNa^+).

UV Measurements. Absorption spectra of all oligonucleotides were determined in PBS buffer (pH 7.4). The concentrations of the oligonucleotides were determined by UV absorption measurement at 260 nm and were found to be at 0.1−5.5 μM range. Absorbance was kept less than 0.5 AU in order to avoid inner filter distortion. Samples were measured in a 10 mm quartz cell.

Fluorescence Measurements. The measurement conditions of oligonucleotides and RNA extracts included 610 V sensitivity and a 4 nm slit. Samples were measured in PBS buffer (pH 7.4). The concentration of the samples was in the range of 0.1−5.5 μM. Samples were measured in a 10 mm quartz cell.

Quantum Yield Measurements. The quantum yield of each oligonucleotide was calculated from the observed absorbance and the area of the fluorescence emission band. The fluorescence quantum yields of all oligonucleotides were determined relative to the quantum yield of quinine sulfate (0.58) in 0.1 M H_2SO_4 according to eq 1.

$$\Phi_F = \Phi_E I/I_R \times OD_R/OD \times \eta^2/\eta_R \quad (1)$$

Where R = reference, I = integration of the peak, and η = refractive index of the solvent.

Hybridization of Oligonucleotides. Solutions of labeled single-strands were mixed at room temperature with an equimolar amount of the complementary single strand oligonucleotides in PBS buffer. Samples were heated to 90 °C for 3−5 min and thereafter annealed by slow cooling to 25 °C.

Melting Temperature Measurements. The T_m values of duplexes were measured in PBS buffer (pH 7) containing 10 mMNaCl and 100 mM phosphate. The absorbance of the samples was monitored at 260 nm from 20 to 85 °C with heating rate of 1 °C/min.

CD Measurements. Circular dichroism (CD) spectra were obtained using a 60 DS CD spectrometer (Aviv Associates, Lakewood, NJ). All measurements were made at 25 °C. Samples were measured in a 10 mm quartz cell. Spectra were obtained in PBS buffer (pH 7) containing 10 mM NaCl and 100 mM phosphate. All spectral data reported here were obtained at a 0.1−0.5 mM concentration of duplex.

Gel Electrophoresis. Agarose gel (1 g) was added to a solution of 100 mL of 0.5% TBE (Tris borate EDTA) in microwave (1 s). The agarose gel was poured into the electrophoresis apparatus and set aside for 20 min for solidification. At this time, the samples were diluted with ethidium bromide and loaded into the gel. The samples were run for 45 min and power setting of 150 V. The concentration of the samples was 0.5 μM.

RNA Cell Extract. Human U2OS osteosarcoma cells were maintained in low glucose Dulbecco's Modified Eagle's Medium (DMEM, Biological Industries, Israel) containing 10% fetal bovine serum (FBS, HyClone, Logan, UT). The clone overexpressing cyclin D1 contained a stable integration of a GFP-cyclin D1 plasmid under the control of the CMV promoter. RNA was extracted from wild-type U2OS cells and cyclin D1 overexpressing cells using TRI Reagent Sigma-Aldrich protocol.

For RT-PCR, DNA-free Kit (Ambion) was used to remove genomic DNA contamination. cDNA (1 μg RNA) was synthesized using the ReverseAid First Strand cDNA Synthesis Kit (Fermentas) with oligo-dT as a primer. Semiquantitative RT-PCR was performed using Eppendorf Thermocycler amplification for 19−38 cycles (depending on the saturation level of the genes amplified) using 1 min denaturation at 94 °C, 1 min annealing at 55 °C for GAPDH and 62 °C for cyclin D1, 1 min extension at 72 °C, and 72 °C for 10 min for final extension. Primers for GAPDH: sense, ACC ACA GTC CAT GCC ATC AC; antisense, TCC ACC ACC CTG TTG CTG TA. Primers for cyclin D1: sense, ATA CTC GAG CCA TGG AAC ACC AGC TCC TGT GC; antisense, GCA ACG AAG GTC TGC GCG TGT TTG C.

Measurements of ODNs in Cell Extract. The measurement conditions of oligonucleotides and RNA extracts included a 610 V sensitivity and a 4 nm slit. Samples were measured in PBS buffer (pH 7.4). The concentration of the samples was 50 μM. Molar ratio of ODN 28 (15:35):complementary ssDNA (35-mer) was 1:5. Samples were measured in a 10 mm quartz cell. All measurements were performed at room temperature.

■ ASSOCIATED CONTENT

Supporting Information

^{1}H, ^{13}C NMR of compounds **9** and **10**, T_m values of dsODN and fluorescence graphs. This material is available free of charge via the Internet at http://pubs.acs.org.

■ AUTHOR INFORMATION

Corresponding Author

*Phone: 972-3-5318303. Fax: 972-3-6354907. E-mail: bilha.fischer@biu.ac.il.

Notes

The authors declare no competing financial interest.

■ ACKNOWLEDGMENTS

We gratefully acknowledge Dr. Gadi Miller for his help in performing a gel electrophoresis experiment.

■ ABBREVIATIONS USED

ODN, oligo deoxynucleic acid; NIF, nucleoside with intrinsic fluorescence; CD, circular dichroism; DMT, 4,4-dimethoxytrityl (4,4′- dimethoxyltriphenylmethyl); PBS, phosphate buffered saline; GAPDH, glyceraldehyde-3-phosphate dehydrogenase

■ REFERENCES

(1) Narihiro, T.; Terada, T.; Ohashi, A.; Wu, J.-H.; Liu, W.-T.; Araki, N.; Kamagata, Y.; Nakamura, K.; Sekiguchi, Y. Quantitative detection of culturable methanogenic archaea abundance in anaerobic treatment systems using the sequence-specific rRNA cleavage method. *ISME J.* **2009**, *3*, 522−535.

(2) Rahaie, M.; Naghavi, M. R.; Alizadeh, H.; Malboobi, M. A.; Dimitrov, K. A novel DNA-based nanostructure for single molecule detection purposes. *Int. J. Nanotechnol.* **2011**, *8*, 458−470.

(3) Pawar, M. G.; Srivatsan, S. G. Synthesis, Photophysical Characterization, and Enzymatic Incorporation of a Microenvironment-Sensitive Fluorescent Uridine Analog. *Org. Lett.* **2011**, *13*, 1114−1117.

(4) Tor, Y. New fluorescent nucleosides for real-time exploration of nucleic acids. *Proc. SPIE—Int. Soc. Opt. Eng.* **2010**, 611−619.

(5) Kimoto, M.; Mitsui, T.; Yokoyama, S.; Hirao, I. A Unique Fluorescent Base Analogue for the Expansion of the Genetic Alphabet. *J. Am. Chem. Soc.* **2010**, *132*, 4988−4989.

(6) Hikida, Y.; Kimoto, M.; Yokoyama, S.; Hirao, I. Site-specific fluorescent probing of RNA molecules by unnatural base-pair transcription for local structural conformation analysis. *Nature Protoc.* **2010**, *5*, 1312−1323.

(7) Bag, S. S.; Kundu, R.; Matsumoto, K.; Saito, Y.; Saito, I. Singly and doubly labeled base-discriminating fluorescent oligonucleotide probes containing oxo-pyrene chromophore. *Bioorg. Med. Chem. Lett.* **2010**, *20*, 3227−3230.

(8) Jiang, D.; Seela, F. Oligonucleotide Duplexes and Multistrand Assemblies with 8-Aza-2′-deoxyisoguanosine: A Fluorescent isoGd Shape Mimic Expanding the Genetic Alphabet and Forming Ionophores. *J. Am. Chem. Soc.* **2010**, *132*, 4016−4024.

(9) Chittepu, P.; Sirivolu, V. R.; Seela, F. Nucleosides and oligonucleotides containing 1,2,3-triazole residues with nucleobase tethers: Synthesis via the azide-alkyne "click" reaction. *Bioorg. Med. Chem. Lett.* **2008**, *16*, 8427−8439.

(10) Gallardo-Escarate, C.; Alvarez-Borrego, J.; Von Brand, E.; Dupre, E.; Del Rio-Portilla, M. A. Relationship between DAPI-

fluorescence fading and nuclear DNA content: an alternative method to DNA quantification? *Biol. Res.* **2007**, *40*, 29−40.
(11) Milanovich, N.; Suh, M.; Jankowiak, R.; Small, G. J.; Hayes, J. M. Binding of TO-PRO-3 and TOTO-3 to DNA: Fluorescence and Hole-Burning Studies. *J. Phy. Chem.* **1996**, *100*, 9181−9186.
(12) Milanovich, N.; Hayes, J. M.; Small, G. J. White light hole burning of TO-PRO-3 bound to oligomeric DNA. *Mol. Cryst. Liq. Cryst. Sci. Technol.* **1996**, *291*, 147−154.
(13) Pribylova, R.; Kralik, P.; Pavlik, I. Oligonucleotide Microarray Technology and its Application to *Mycobacterium avium* subsp. paratuberculosis Research: A Review. *Mol. Biotechnol.* **2009**, *42*, 30−40.
(14) Arvey, A.; Hermann, A.; Hsia, C. C.; Ie, E.; Freund, Y.; McGinnis, W. Minimizing off-target signals in RNA fluorescent in situ hybridization. *Nucleic Acids Res.* **2010**, *38*, 111−117.
(15) Wabuyele, M. B.; Soper, S. A. PCR amplification and sequencing of single copy DNA molecules. *Single Mol.* **2001**, *2*, 13−21.
(16) Beer, C.; Wirth, M. A new method for the quantitative determination of enveloped viral particles. Animal Cell Technology Meets Genomics: Proceedings of the 18th ESACT Meeting, Granada, Spain, May 11−14, 2003; pp 321−324
(17) Ramshesh, V. K.; Knisley, S. B. Use of light absorbers to alter optical interrogation with epi-illumination and transillumination in three-dimensional cardiac models. *J. Biomed. Opt.* **2006**, *11*, 1−12.
(18) Langer, P. R.; Waldrop, A. A.; Ward, D. C. Enzymic synthesis of biotin-labeled polynucleotides: novel nucleic acid affinity probes. *Proc. Natl. Acad. Sci. U. S. A.* **1981**, *78*, 6633−7.
(19) Femino, A. M.; Fay, F. S.; Fogarty, K.; Singer, R. H. Visualization of single RNA transcripts in situ. *Science* **1998**, *280*, 585−590.
(20) Levsky, J. M.; Braut, S. A.; Singer, R. H. Single Cell Gene Expression Profiling: Multiplexed Expression Fluorescence in situ Hybridization (FISH). *Singer Lab Protocol*, Apr 30, 2003; http://www.einstein.yu.edu/uploadedFiles/LABS/robert-singer-lab/profiling.pdf.
(21) Dodd, D. W.; Hudson, R. Intrinsically fluorescent base-discriminating nucleoside analogs. *Rev. Org. Chem.* **2009**, *6*, 378−391.
(22) Sirivolu Venkata, R.; Chittepu, P.; Seela, F. DNA with branched internal side chains: synthesis of 5-tripropargylamine-dU and conjugation by an azide-alkyne double click reaction. *Eur. J. Org. Chem.* **2008**, *9*, 2305−2316.
(23) Hudson, R. H. E.; Ghorbani-Choghamarani, A. Oligodeoxynucleotides incorporating structurally simple 5-alkynyl-2′-deoxyuridines fluorometrically respond to hybridization. *Org. Biomol. Chem.* **2007**, *5*, 1845−1848.
(24) Hudson, R.; Moszynski, J. M. A facile synthesis of fluorophores based on 5-phenylethynyluracils. *Synlett* **2006**, 2997−3000.
(25) Hudson, R. H. E.; Dambenieks, A. K. Synthesis of N1-unsubstituted 5-alkynyl-cytosine and derivatives thereof. *Heterocycles* **2006**, *68*, 1325−1328.
(26) Wilhelmsson, L. M.; Holmen, A.; Lincoln, P.; Nielsen, P. E.; Norden, B. A Highly Fluorescent DNA Base Analogue that Forms Watson−Crick Base Pairs with Guanine. *J. Am. Chem. Soc.* **2001**, *123*, 2434−2435.
(27) Peter, S.; L. Marcus, W.; Per, L.; Vicki, E.; Tom, B.; Bo, A. Fluorescent properties of DNA base analogue tC upon incorporation into DNA—negligible influence of neighbouring bases on fluorescence quantum yield. *Nucleic Acids Res.* **2005**, *33*, 5019−5025.
(28) Peter, S.; Gudrun, S.; Thomas, L.; Karl, B.; Bertil, M.; Marcus, W. Highly efficient incorporation of the fluorescent nucleotide analogs tC and tCO by Klenow fragment. *Nucleic Acids Res.* **2009**, *37*, 3924−3933.
(29) Karl, B.; Peter, S.; Marcus., L. Nucleic acid structure and sequence probing using fluorescent base analogue tCO. *Biophys. Chem.* **2009**, *139*, 24−28.
(30) Preus, S.; Kilsa, K.; Wilhelmsson, L. M.; Albinsson, B. Photophysical and structural properties of the fluorescent nucleobase analogues of the tricyclic cytosine (tC) family. *Phys. Chem. Chem. Phys.* **2010**, *12*, 8881−8892.
(31) Mizuta M, M. K.; Seio, K.; Santa, T.; Sekine, M. Synthesis of fluorescent cyclic cytosine nucleosides and their fluorescent properties upon incorporation into oligonucleotides. *Nucleic Acids Symp. Ser.* **2006**, *50*, 19−20.
(32) Mizuta, M.; Seio, K.; Miyata, K.; Sekine, M. Fluorescent Pyrimidopyrimidoindole Nucleosides: Control of Photophysical Characterizations by Substituent Effects. *J. Org. Chem.* **2007**, *72*, 5046−5055.
(33) Durand, M.; Maurizot, J. C.; Asseline, U.; Barbier, C.; Thuong, N. T.; Helene, C. Oligothymidylates covalently linked to an acridine derivative and with modified phosphodiester backbone: circular dichroism studies of their interactions with complementary sequences. *Nucleic Acids Res.* **1989**, *17*, 1823−37.
(34) Segal, M.; Fischer, B. Analogues of Uracil Nucleosides with Intrinsic Fluorescence (NIF-analogues). Synthesis and Photophysical Properties. *Org. Biomol. Chem.* **2012**, *2012*, 1571−1580.
(35) Johnson, D. G.; Walker, C. L. Cyclins and cell cycle checkpoints. *Annu. Rev. Pharmacol. Toxicol.* **1999**, *39*, 295−312.
(36) Bates, S.; Peters, G. Cyclin D1 as a cellular proto-oncogene. *Semin. Cancer Biol.* **1995**, *6*, 73−82.
(37) Arnold, A.; Papanikolaou, A. Cyclin D1 in breast cancer pathogenesis. *J. Clin. Oncol.* **2005**, *23*, 4215−4224.
(38) Bertrand, E.; Chartrand, P.; Schaefer, M.; Shenoy, S. M.; Singer, R. H.; Long, R. M. Localization of ASH1 mRNA particles in living yeast. *Mol. Cell* **1998**, *2*, 437−445.
(39) Yunger, S.; Rosenfeld, L.; Garini, Y.; Shav-Tal, Y. Single-allele analysis of transcription kinetics in living mammalian cells. *Nature Methods* **2010**, *7*, 631−633.
(40) Sun, S.; Li, W.; Sun, Y.; Pan, Y.; Li, J. A new RNA vaccine platform based on MS2 virus-like particles produced in *Saccharomyces cerevisiae*. *Biochem. Biophys. Res. Commun.* **2011**, *407*, 124−128.
(41) Cohen, B. A.; Kaloyeros, A. E.; Bergkvist, M. MS2 bacteriophage as a delivery vessel of porphyrins for photodynamic therapy. *Proc. SPIE—Int. Soc. Opt. Eng.* **2011**, *7886*, 1−7.
(42) Guo, Z. Y.; Hao, X. H.; Tan, F. F.; Pei, X.; Shang, L. M.; Jiang, X. L.; Yang, F. The elements of human cyclin D1 promoter and regulation involved. *Clin. Epigenet.* **2011**, *2*, 63−76.
(43) Engman, K. C.; Sandin, P.; Osborne, S.; Brown, T.; Billeter, M.; Lincoln, P.; Norden, B.; Albinsson, B.; Wilhelmsson, L. M. DNA adopts normal B-form upon incorporation of highly fluorescent DNA base analogue tC: NMR structure and UV−vis spectroscopy characterization. *Nucleic Acids Res.* **2004**, *32*, 5087−5095.
(44) Jiang, H.; Gao, Q.-R.; Li, L.-J.; Kong, L.-R.; Zhang, W.-D.; Wu, S.-W.; Yang, Y.-L. Genetic diversity of recurrent selection populations with Ms2 gene assessed by gliadins in common wheat (*Triticum aestivum* L.). *Agric. Sci. Chin.* **2010**, *9*, 615−625.
(45) Wei, M.; Zhu, L.; Li, Y.; Chen, W.; Han, B.; Wang, Z.; He, J.; Yao, H.; Yang, Z.; Zhang, Q.; Liu, B.; Gu, Q.; Zhu, Z.; Shen, K. Knocking down cyclin D1b inhibits breast cancer cell growth and suppresses tumor development in a breast cancer model. *Cancer Sci.* **2011**, *102*, 1537−1544.
(46) Sandin, P.; Boerjesson, K.; Li, H.; Martensson, J.; Brown, T.; Wilhelmsson, L. M.; Albinsson, B. Characterization and use of an unprecedentedly bright and structurally non-perturbing fluorescent DNA base analogue. *Nucleic Acids Res.* **2008**, *36*, 157−167.
(47) Shin, D.; Sinkeldam, R. W.; Tor, Y. Emissive RNA Alphabet. *J. Am. Chem. Soc.* **2011**, *133*, 14912−14915.
(48) Greco, N. J.; Tor, Y. Simple Fluorescent Pyrimidine Analogues Detect the Presence of DNA Abasic Sites. *J. Am. Chem. Soc.* **2005**, *127*, 10784−10785.